38th European Rotorcraft Forum, Paper 2012-129.
September 4-7 2012, Amsterdam, The Netherlands

European Rotorcraft Forum

A REDUCED ORDER METHODOLOGY FOR THE PARAMETRIC ANALYSIS OF ROTOR AERODYNAMICS

Marco Fossati, marco.fossati@cfdlab.mcgill.ca, McGill University (Canada)
Wagdi G. Habashi, wagdi.habashi@mcgill.ca, McGill University (Canada)
Massimo Biava, biava.awparc@agustawestland.com, AWPARC (Italy)
Luigi Vigevano, luigi.vigevano@polimi.it, Politecnico di Milano (Italy)

Abstract

A reduced order methodology, based on Proper Orthogonal Decomposition (POD) and multidimensional interpolation, is proposed for the parametric study of rotor flows under hovering conditions. The POD-based methodology makes no simplification of the complexity of the three-dimensional, viscous turbulent flow generated by the rotor but still yields accurate solutions at a fraction of the time required by standard CFD. The use of interpolation techniques other than projection operators allows dealing in a unified manner with experimental data, CFD computations or a combination of both. The method provides fast and accurate solutions for local flow details and integral quantities like aerodynamic coefficients. The POD-based methodology is demonstrated to have a multiplier effect on wind tunnel and CFD simulations of rotorcraft aerodynamics and as a potential powerful methodology to construct a new generation of rotorcraft simulators.

1. INTRODUCTION

The evaluation of the aerodynamic performance of an isolated rotor is a critical step in the design process of a rotorcraft. The main rotor is the only source of thrust; it is the means by which a horizontal propulsive force can be generated and it allows creating forces and moments to control the attitude and position of the rotorcraft [1,2]. Many decisions at the design level depend on the assessment of the rotor aerodynamics and in order to gather as much information as possible, the rotor flow has to be evaluated for many different geometrical configurations and operating conditions. The complexity of the rotor's flow field makes experiments difficult, expensive and limited to a narrow operational matrix [3-5]. Numerical modeling is a valid alternative/complement to wind tunnel tests. Unfortunately, Computational Fluid Dynamics (CFD) techniques, in the form of three-dimensional turbulent Navier-Stokes computations are, at the present time, still too demanding in terms of computing power to be used extensively in the design process [6-8].

Simplified analytical, semi-empirical and numerical methods have been proposed in the literature as an alternative to full viscous-turbulent CFD simulations [9-12]. These methods are loosely labeled Reduced Order Methods (ROM) to indicate the reduced computational complexity compared to standard CFD. Classical approaches based on momentum and/or blade element theory are often, if not always, used for preliminary estimates of thrust and moment. These estimates can be refined using vortex methods in conjunction with lifting-line, lifting-surface, or panel methods to calculate the strength of the wake and other important aerodynamic parameters. Unfortunately, the majority of these simplified methods are not general enough to describe the complex three-dimensional viscous flow in the rotor wake and do not provide the required level of accuracy for the operating conditions that should be analyzed.

In recent years, a new category of Reduced Order methodologies has become popular in the context of computational physics and engineering. This is a class of techniques that makes no simplification as to the geometry of the problem (1D or 2D) or the physics of the flow (inviscid, incompressible, etc.), but introduces the use of the eigenmodes of the viscous-turbulent flow field to reformulate the original system of PDEs in a computationally more tractable manner [13-15]. These techniques are generally referred to as Reduced Basis Methods (RBM), and their underlying principle is to obtain a simplification of the problem in terms of a reduction of the number of degrees of freedom rather than by sacrificing the physics of the problem. Reduction with RBMs is effective only when it is possible to identify, in a controlled manner, a limited number of eigenmodes (a few dozens or less) that allow representing if not all then at least most of the energy contained in the original system.

The ROM methods based on flow modal analysis use a number of observations (snapshots) of the system computed (or measured) at different operating conditions to identify the dominant physics of the problem, i.e. its eigenmodes. These allow defining a vector space where the solution of the

system for an unsolved (or untested) condition can be obtained as a combination of these fundamental solutions. RBM methods can be classified into two different categories: intrusive and non-intrusive RBMs. Intrusive methods compute the coefficients of the combination for the unknown state by solving a reduced system of equations obtained by projecting in a (Petrov-) Galerkin sense the original PDEs on the eigenmodes [16,17]. Non-intrusive approaches on the other hand circumvent the projection phase by making use of other approaches to get the reduced solution [18,19]. A popular technique used in non-intrusive approaches is interpolation of coefficients. Originally proposed by Ly [20] and Bui-Than [21], and recently developed by Fossati et al [22, 23], the RBM with interpolation (hereinafter RBMI) gets the coefficients for the solution at an unknown state by interpolating the known modal coefficients used to reconstruct the snapshots.

In the context of rotorcraft engineering and design, approaches that use information from an available set of CFD solutions have been studied in the last decade. In the recent literature, these are referred to as surrogate methods and have been primarily adopted to get integral quantities like aerodynamic coefficients and loads [24-26]. These approaches are essentially based on response surface methods (RSM) and neural networks (NN). In other words these methods attempt to define an input-output mapping between the operating conditions (i.e. Mach number and/or the kinematic parameters of the rotor) and the desired output such as lift, drag and moment coefficients. A first attempt to use RBM in reproducing a 3D flow field is documented in the work of Tang [27]. In his work, the eigenvalues of the aerodynamic field were extracted from a simplified 3D representation of the rotor wake and only a few of them were eventually used to reproduce the complete induced flow from the rotor disk. To the best of the authors' knowledge, no follow up to this work has been proposed in the recent literature.

In the present work, a non-intrusive RBM approach is described and evaluated for its capability to address both local flow field features and integral aerodynamic quantities. It is applied to the problem of the steady flow through an isolated rotor in the context of a parametric analysis. The approach adopted here is the one proposed by Fossati et al [22, 23]. It had been originally developed for the parametric analysis of aero-icing problems, but has recently been successfully applied to unsteady vortex-dominated flows around fixed wing high-lift configurations [28]. The attractive feature of this non-intrusive approach is that it allows a "black-box" evaluation of aerodynamic data. This allows fulfilling two goals: 1) reduction will be realized at the CFD level by reducing the computational cost and at the experimental level by reducing the number of tests and/or the complexity of the mock-up in terms of areas to be instrumented, 2) it will permit keeping together experimental data and high-fidelity CFD simulations to get the most complete picture of the problem under investigation.

The discussion is organized as follows. In the first section, the RBM approach based on Proper Orthogonal Decomposition and interpolation will be outlined. Starting from section three, the assessment of the method will be presented considering first the ability of the POD-based method to reproduce and enrich experimental data. Eventually, the performance of the ROM method will be validated against high-fidelity CFD simulations in terms of local flow features and integral quantities.

2. REDUCED BASIS MODELING: POD AND INTERPOLATION

A detailed description of the method is outside the scope of the present work where the focus is more on the application and assessment side. For self-containment, a brief description is reported here. The interested reader is referred to [21-23].

The methodology is composed of three phases:

1. Identification and computation (measurement) of the snapshots of the system
2. Extraction of the eigenmodes of the flow via Proper Orthogonal Decomposition
3. Computation of the coefficients for the combination of modes

Phases 1 and 2 define what is referred to as the off-line part. Snapshots are identified and computed (or measured) once and for all. This is the most cost-intensive part since it requires high-fidelity CFD or wind tunnel data. Phase 2 is also an off-line part since once the set of snapshots is obtained, the eigenmodes can be uniquely computed and these will remain the same as long as the set of snapshots does not change. Note that at this point it could be possible to subdivide the snapshots in sub-sets and perform modes extraction separately for each one of these groups. This approach could result in increased accuracy since snapshots with similar behavior can be grouped together and provide a local RBM to account for small variations in limited regions of the parameter space. Nevertheless, the definition of a consistent method to select how many and which snapshots should be grouped together is a non-trivial problem, especially in cases where the snapshots are a combination of CFD and experimental data. In the present method, a global approach has been adopted instead, where a unique set of eigenmodes is obtained over the entire

parameter space using all the snapshots.

Phase 3 is the actual on-line step. This is the part where the unknown solution is computed by interpolation of the modal coefficients. For all the tests presented in the later sections of the paper an indication of both the off-line and on-line time will be provided, with two observations: 1) in the case of experimental data, no information was available to the authors to assess the time required to perform a single wind tunnel test, 2) the time required for the eigenmodes extraction is typically a few seconds if not a fraction of a second, hence it does not provide any kind of overhead to the global cost.

In the following two sections, phase 2 and 3 will be described. Phase 1 can be recast as a problem in the area of the Design of (Computer) Experiments and it deals with the problem of identifying the best sampling of the parameter space for which the problem has to be analyzed. In the case of experimental data, the authors had no choice other that to take the snapshots as these were defined in the original experiments. In the case of the CFD-based RBMI, a technique based on Centroidal Voronoi Tessellation [30] could be adopted to cluster the samples (i.e. the points for which a CFD solutions had to be computed) in the regions of supposed high nonlinearities.

2.1. Eigenmodes extraction: Proper Orthogonal Decomposition

Proper Orthogonal Decomposition (POD) is referred to in different ways according to the context where it is introduced. Common identifiers are: the Singular Value Decomposition or the Karhunen-Loëve decomposition [31]. The method can be applied to non-linear problems and its ability to isolate the dominant features of complex dynamical systems has been exploited in fundamental studies of the dynamics of fluids [32,33]. The attractive feature of POD in the context of RBMs is its ability to provide explicit control on the minimum number of modes required to represent most, if not all, of the energy of the original full-order system. This “error-bounded“ truncation of the POD modes to the most energetic ones has made this technique very popular in the engineering context and it constitutes the basis of many RBMs. POD processes a set of available observations of the system and for highly nonlinear problems it can require a significant amount of computational resources [31]. Since computational complexity is of main concern in any ROM technique, the method of snapshots proposed by Sirovich is used to perform the eigenmodes extraction [33].

Let us assume the existence of an ensemble of N_S observations $\boldsymbol{U} \in \mathbb{R}^{N_S \times N_P}$. Each observation of the system can be written as $\boldsymbol{U}_j \in \mathbb{R}^{N_P}\ j = 1, \cdots, N_S$, where N_P is the number of points for which the observation is defined, i.e. the number of grid points in the case of a CFD solution or the number of probe points in an experiment. The target is to find a set of basis vectors $\boldsymbol{\phi} \in \mathbb{R}^{N_S \times N_P}$ that best represents the snapshots, according to the following maximization problem:

$$\max_{\boldsymbol{\psi}} \langle (\boldsymbol{U}, \boldsymbol{\psi}) \rangle / (\boldsymbol{\psi}, \boldsymbol{\psi}) = \langle (\boldsymbol{U}, \boldsymbol{\phi}) \rangle / (\boldsymbol{\phi}, \boldsymbol{\phi}) \tag{1}$$

where the square brackets $\langle \cdot \rangle$ indicate time averaging and the operator $(\cdot,\cdot)$ indicates an inner product. It can be shown that the desired eigenfunctions $\boldsymbol{\phi}$ can be computed as a combination of the snapshots $\boldsymbol{U}_j$ of the system, i.e.

$$\boldsymbol{\phi}_i = \sum_{j=1}^{N_S} \boldsymbol{\beta}_j^i \ \boldsymbol{U}_j \qquad i = 1, \cdots, N_S \tag{2}$$

and as a result, the problem of finding N_S functions $\boldsymbol{\phi}_i$ can be recast as an eigenvalue-eigenvector problem $R\boldsymbol{\beta} = \lambda\boldsymbol{\beta}$, where R is a correlation matrix defined in terms of the scalar products between snapshots

$$R_{ij} = \left(\boldsymbol{U}_i, \boldsymbol{U}_j\right)/N_S \qquad i, j = 1, \dots, N_S \tag{3}$$

The eigenvectors $\boldsymbol{\beta}$ give the POD modes via equation (2), while the eigenvalues $\boldsymbol{\lambda}$ give the fraction of total energy associated to each mode $\boldsymbol{\phi}_i$

$$E_i = \lambda_i / \sum_{i=1}^{Ns} \lambda_i \tag{4}$$

The POD prediction of the state of the system at any unknown condition will read

$$\boldsymbol{V} = \sum_{j=1}^{M \le N_S} \alpha_j \, \boldsymbol{\phi}_j \tag{5}$$

where M indicates the truncation of the expansion at the desired level of energy content.

2.2. Solution of the reduced order model: Interpolation of coefficients

Equation (5) can be used to compute the state of the system at a specific location $\boldsymbol{\delta}$ in the parameters space. The modes are known from equation (2) and the only unknowns left are the $M \le N_S$ coefficients $\boldsymbol{\alpha}^{\boldsymbol{\delta}} = \boldsymbol{\alpha}(\boldsymbol{\delta})$. Since the snapshots can themselves be written as a combination of the eigenfunctions $\boldsymbol{\phi}_i$, it is possible to compute the coefficients α_j associated to each snapshot as follows

$$\alpha_j = \left(\boldsymbol{U}_j, \boldsymbol{\phi}_j\right) \qquad j = 1, \cdots, N_S \tag{6}$$

The desired $\boldsymbol{\alpha}^{\boldsymbol{\delta}}$ can be obtained by creating a multidimensional response surface having as input

the parameters (i.e. the operational conditions) of the analysis and the α_j coefficients as output.

Different interpolation techniques are considered: the Akima interpolation method [34] and techniques based on the Kriging method [35]. Akima is a very efficient method but is practical only for a maximum of two parameters. Kriging, on the other hand, can be used with more than two parameters and performs well with non-smooth functions. The Ordinary Kriging formula reads

$$\alpha_j(\boldsymbol{\delta}) = \gamma + \boldsymbol{\psi}^T \boldsymbol{\Psi}^{-1}(\boldsymbol{\alpha} - \mathbf{1}\gamma) \quad j = 1, \dots, M \leq N_S \tag{7}$$

where the matrix $\Psi_{i,j} = \psi(\boldsymbol{x}^i, \boldsymbol{x}^j) = \exp[-(\boldsymbol{\theta}^T(\boldsymbol{x}^i - \boldsymbol{x}^j)^2)]$, $\gamma = (\mathbf{1}^T\boldsymbol{\Psi}^{-1}\boldsymbol{\alpha})/(\mathbf{1}^T\boldsymbol{\Psi}^{-1}\mathbf{1})$ and $\boldsymbol{x}^i$ represents the location of the i^{th} snapshot in the parameter space. The Ordinary Kriging formula (7) represents the unknown coefficients as a sum of a constant global model γ plus a perturbation based on Gaussian statistical considerations [23,35]. The interpolation formula filters the assumption that "vicinity in the parameter space implies similarity of the coefficients" on the basis of the weight $\boldsymbol{\theta}$. The vector $\boldsymbol{\theta} \in \mathbb{R}^{N_D}$ with N_D equal to the number of parameters, is an unknown model parameter determined by maximizing the likelihood function [35]

$$Ln = -\frac{1}{2}\left[N_S \ln(\sigma^2) + ln|\boldsymbol{\Psi}|\right] \tag{8}$$

Here $\sigma^2 = 1/N_S\,(\boldsymbol{\alpha} - \mathbf{1}\gamma)^T\,\boldsymbol{\Psi}^{-1}(\boldsymbol{\alpha} - \mathbf{1}\gamma)$.

A recent variant of the Ordinary Kriging method, referred to as Bayesian Kriging [36], has also been considered for its ability to deal with highly nonlinear response surfaces. Bayesian Kriging generalizes the Ordinary Kriging method by adding nonlinear terms to the original interpolation formula, i.e.

$$\alpha_j(\boldsymbol{\delta}) = \boldsymbol{v}(\boldsymbol{\delta})^T\boldsymbol{\gamma}_B + \boldsymbol{\psi}^T\boldsymbol{\Psi}^{-1}(\boldsymbol{\alpha} - \boldsymbol{V}_B\boldsymbol{\gamma}_B) \tag{9}$$

Here $\boldsymbol{v}(\boldsymbol{\delta}) = \{1, v_1(\boldsymbol{\delta}), \dots, v_B(\boldsymbol{\delta})\}$ are $B+1$ unknown scalar functions whose form and number (B) will be determined on the basis of Bayesian statistics considerations. $\boldsymbol{V}_B$ is a $N_S \times (B+1)$ matrix whose first column is 1 and the b-th column is made by the evaluation of the b-th unknown scalar function for each snapshot's location $v_b(\boldsymbol{x}^i)$. The scalar constant model γ is replaced by a non-constant vector term $\boldsymbol{\gamma}_B$

$$\boldsymbol{\gamma}_B = (\boldsymbol{V}_B^T\boldsymbol{\Psi}^{-1}\boldsymbol{V}_B)^{-1}(\boldsymbol{V}_B^T\boldsymbol{\Psi}^{-1}\boldsymbol{\alpha}) \tag{10}$$

The number of new terms $(B+1)$ and their form $(\boldsymbol{v}(\boldsymbol{\delta}) = \{1, v_1(\boldsymbol{\delta}), \dots, v_B(\boldsymbol{\delta})\})$ are defined according to the highest probability (in the Bayesian sense) of improving the accuracy of the interpolation [23,36].

3. RBM BASED ON EXPERIMENTAL DATA

Precise and accurate measurements of the rotor flow have become more and more common in the last years. However, the amount of data to be processed in this activity is staggering and moreover the complexity of wind tunnel models and the cost of these experimental campaigns are not always affordable. In this section, the RBMI methodology is applied directly to data acquired in wind tunnel tests. The goal is to assess the method's efficiency 1) in reducing the number of probes to be placed in the model and 2) in limiting the number of operational conditions to be tested.

3.1. Caradonna-Tung experiment

A very well known experimental campaign on isolated rotors is the one from Caradonna and Tung [3]. An isolated rotor with untapered and untwisted blades of NACA0012 sections has been instrumented with pressure probes at multiple locations along the blade chord and at multiple sections of the blade (r/R). Each blade has been instrumented at five different sections: r/R = 0.5, 0.68, 0.8, 0.89 and 0.96. A total of 32 different operating conditions have been tested for different values of the angular velocity (ω) and the collective pitch angle (α). A total of 32 x 5 = 160 observations are available form the Caradonna Tung campaign. The pitch varies from 0 degrees to 12 degrees and the rotational speed ranges from 650 to 2540 rpm. The Mach number at the tip of the blade for the tested conditions ranges from 0.226 to 0.815, that is from subsonic to transonic and, as a result, the snapshots are characterized by a sensible variability in the pressure coefficients curves, ranging from smooth distributions to curves with steep gradients as shock waves appears in the transonic regime. Figure 1 shows the geometry of the problem and the runs arrangement in the α-ω plane.

The present RBM method can work only with data that has a homogeneous number of points (in this case pressure probes) among the snapshots. Since the number of probes used in the experiments is different at the different sections, the C_p profiles have been interpolated along each section to give a distribution of 320 points along each section and on the upper and lower surface of the blade. Akima has been used for the preprocessing of the data.

3.2. RBM for mock-up simplification

The first test is an assessment of the RBM approach to evaluate the possibility of reducing the number of instrumented sections along the blade. The C_p data along two of the five sections have been excluded from the available set, reducing the number of snapshots to 96. This approach mimics the case of a

blade that has been instrumented only along three sections instead of five. The data at r/R = 0.68 and r/R = 0.89 have been removed from the set. The omitted 64 C_p distributions have been obtained with the RBM method. Two arbitrarily selected operating conditions (indicated as targets of the RBM) are reported here to show the effectiveness of the method. These are summarized in table 1. The energy threshold adopted for the POD modes extraction is 99.9%resulting in the selection of 12 modes for the upper surface and only 6 modes for the lower one.

	r/R	ω [rpm]	α [°]	$Mach_{TIP}$
Target A	0.68, 0.89	1250	8	0.439
Target B	0.68, 0.89	2268	5	0.794

Table 1: Target solutions for the mock-up simplification test case.

Figures 2 and 3 illustrate the comparison of the RBM solutions at the omitted sections with the reference experimental Cp data. A Bayesian Kriging method of order zero, i.e. Ordinary Kriging, has been automatically selected as the best interpolation formula and each target required few seconds to execute.

3.3. RBM for reducing the number of wind tunnel tests

The second test introduces an additional reduction of the problem by reducing the number of tests to be run in the wind tunnel. To this end, the entire row of runs corresponding to a pitch of 8 degrees has been removed from the data. This operation mimics the condition where, in addition to having only three sections instrumented instead of five; only 21 runs have been performed instead of 32. The total number of snapshots in this case is 63 (recall that originally these were 160). Two targets are reported here to show the performance of the method in this case. Operating conditions are indicated in table 2.

	r/R	ω [rpm]	α [°]	$Mach_{TIP}$
Target C	0.68, 0.89	1250	8	0.439
Target D	0.68, 0.89	2400	8	0.845

Table 2: Target solutions for the wind tunnel runs reduction test case.

Target C is the same as target A and it allows showing the difference between the two different sets of data used to build the RBM model. Target D has been chosen instead to be close to the boundary of the parameter space such that the performance of the method in regions that are typically troublesome for interpolation techniques can be assessed. An energy level of 99.9% has been selected and 10 modes have been extracted for the upper surface while only 5 modes have been selected for the lower surface. Figures 4 and 5 show the results of the analysis. A comparison between figure 2 and figure 4 shows minor differences between the C_p curves, mainly in correspondence of the peak value of C_p. The entire RBM computation takes again few seconds on a single CPU. It is observed that for the subsonic regime the agreement between the RBM and the experimental data is very good, while in the case of transonic conditions a visible discrepancy is observed in the proximity of the shock wave. In this case the Bayesian Kriging of order three, i.e. with three new terms added to the Ordinary Kriging formula was the method capable of providing the most accurate results.

4. RBM BASED OF HIGH-FIDELITY CFD DATA

CFD modeling and simulation of rotor flow has given a great momentum to the analysis of the aerodynamics of rotorcraft, but require significant computational resources. That is why, still today approximate methods are widely used in many design phases. The coupling of the present RBMI method with CFD data is the natural environment where information about the entire flow field around a rotor can be obtained with good accuracy at a marginal computational cost. In this section the effectiveness of the RBMI in computing local phenomena as well as integral quantities is assessed.

4.1. The CFD solver ROSITA

The high-fidelity CFD solutions have been obtained using the solver ROSITA [6]. The RANS equations are integrated numerically over a system of moving, overset, multi-block grids. The one-equation Spalart-Allmaras turbulence model is used. The equations are discretized in space using a cell-centered finite-volume implementation of the Roe scheme [37]. Second order accuracy is obtained by MUSCL extrapolation supplemented with the version of the Van Albada limiter introduced by Venkatakrishnan [38]. The viscous terms are computed by the application of the Gauss theorem and using a cell-centered discretization scheme. Time integration is carried out with a dual-time stepping formulation [39] that uses a second order backward differentiation formula and a fully unfactored implicit scheme in pseudo-time. The generalized conjugate gradient method is used to solve the linear system, in conjunction with a block incomplete lower-upper preconditioner.

The connectivity between the (possibly) moving grids is computed by means of a modified Chimera technique proposed by Chesshire and Henshaw [40]. The integration of the aerodynamic forces on overlapping surfaces is performed using the methodology proposed by Chan and Buning [41]. The parallel implementation of ROSITA is based on the message passing programming paradigm (MPI), and the parallelization strategy consists in distributing the overset blocks among the available processors to obtain an optimal load balancing.

4.2. Parametric study of the ONERA-7AD rotor

The parametric study of the steady flow around the four bladed ONERA 7AD rotor is addressed. Each blade has an aspect ratio of 15 and consists of airfoils of the OA2XX series, with parabolic taper at the blade tip and an anhedral angle [4,6]. Two parameters have been chosen for the analysis: Mach number at blade tip and collective pitch at r/R = 0.75. The operational range considered in the present analysis is summarized in table 3.

Pitch @ r/R = 0.75	2.0	14.0
Mach @ blade tip	0.5	0.7

Table 3: Parameter space for the ONERA 7AD rotor.

A matrix of 22 CFD tests have been identified adopting a sampling method called Centroidal Voronoi Tessellation [30]. Points have been clustered in the region of high pitch and high Mach number, since this is the region where complex flow features, like separation and/or strong gradients are expected to occur. The blades are assumed to be rigid bodies and for each one of the 22 different Mach and pitch values, a suitable flap angle has been defined on the basis of an estimated balance between the centrifugal force, the weight and the lift along the blade. No rotation has been applied around the lead-lag hinge. Symmetry has been used to reduce the cost and only one blade with periodic boundary conditions has been simulated. The multi-block Chimera mesh is made of 1 single-block background mesh together with one multi-block (4 blocks) mesh around the blade. Figure 6 shows the system of grids. The background mesh is made of 1'624'320 elements while the multi-block mesh is made of 1'389'240 elements. Each CFD simulation required approximately 2 hrs on 72 Intel Xeon 2.4GHz CPUs with infiniband connection. Figure 7 shows the location of the CFD solutions in the parameters space.

4.3. RBM for the entire flow field

The RBM model is built by choosing a threshold of 99.9% for the energy content. This led to the identification of 13 modes to be used in the definition of the reduced solution. In this case, the leave-one-out methodology has been used for estimating the accuracy of the reduced model at the snapshots locations. Iteratively, each snapshot is excluded from the dataset used to build the RBM and it is subsequently adopted as a reference solution to compute the error of the RBM solution. The L_2 norm of the field error has been computed for the pressure (P) and the components of the shear stress vector (τ_x, τ_y, τ_z). The error at the snapshots locations is taken as the maximum of the error for each field

$$L_\infty = \max\{L_{2,P}, L_{2,\tau x}, L_{2,\tau y}, L_{2,\tau z}\} \tag{11}$$

The choice of the static pressure and the shear stress vector as the variables to define the error is motivated by the interest using the RBMI approach to eventually get the aerodynamic loads on the rotor. The leave-one-out approach to error estimation does not give rigorous error bounds but provides only a gross estimate of the accuracy of the RBMI model on the basis of a depleted set of snapshots. RBMs based on projection allow for more accurate error as a consequence of the more rigorous mathematical reformulation of the PDEs [29]. The left part of figure 8 shows the eigenvalue convergence with the threshold level selected. The right part of the figure presents the distribution of the error in the parameter space. A smooth distribution has been obtained by interpolating the error values of the snapshots.

Two targets have been identified in the parameter space. The first one is the well-known HELISHAPE case [4,6] and the second one has been arbitrarily selected to be in a region of high error to assess more precisely the error on the reduced solution. Table 4 summarizes the conditions for these two targets and figure 7 shows their location in the parameter space. Two additional CFD runs have been performed with the solver ROSITA to get the reference solutions for comparison.

	Pitch	Mach_{TIP}
Target E (HELISHAPE)	7.5	0.662
Target F	13.0	0.654

Table 4: Targets for the ONERA 7AD case.

Figures 9 to 12 illustrate the comparison between the RBMI and the CFD solution for the selected targets. Remarkable agreement is observed in the case of the HELISHAPE conditions where the difference between the Cp profiles at r/R = 0.915 is hardly visible. A marked difference is instead observed for target F in figure 11. Each RBMI computation of the entire computational domain takes approximately 35 seconds on a single CPU where a CFD solution takes 2 hours on 72 CPUs.

Akima and Kriging interpolation methods are both applicable for this two-parameter problem. No significant differences have been observed between the methods; hence Akima has been used for the rest of the analysis due to its lower computational cost compared to Kriging. Figure 10 and 12 show the comparison of the tip vortex trajectory as visualized by the Q-criterion. The comparison is satisfactory. In the case of target F, some numerical artifacts are observed near blade tip and the tip vortex coming from the preceding blade is not reconstructed in its entirety. However, the fair agreement observed by the application of the Q-criterion supports the adoption of the RBMI method for the identification of vortical structures that characterize the aerodynamic and aeroacoustics of the rotor in the context of parametric analyses.

4.4. RBM for integral quantities

As a final test, the ROM methodology is used to obtain information about integral quantities. It is important to observe that the natural context of the present ROM method is in the derivation of complex flow fields and the computation of integral quantities is intended as a post-processing of the "reduced fields". This is worth noting because the present method, when applied directly to integral quantities like, thrust (Ct) or torque (Cq) coefficients, reduces to pure interpolation, so no marked advantage with respect to other surrogate methods (RSM, NN, etc.) is obtained in this case. On the contrary, if integrals are computed as a post-processing of reduced local flow field quantities, superior robustness and accuracy are expected due to the ability to incorporate the physics of the problem via the POD modes.

The integral quantity considered is the Figure of Merit (FoM). The FoM is a quantity that describes the ratio between the ideal power and the actual power necessary to obtain that thrust. The left part of figure 13 shows the contours of the FoM as obtained from ROSITA. The highest values of the FoM are obtained for high values of collective pitch and low-to-moderate values of the Mach number. As the Mach number (i.e. the rotational speed) gets higher, the increase in the aerodynamic drag becomes predominant over the increase in lift, and a reduction in the FoM is observed.

To obtain a complete investigation of the rotor FoM on the parameter space, 1076 points, each corresponding to a specific pair of Pitch and Mach (and flap angle), have been identified via CVT. The set of 22 snapshots has been used to compute the 1076 RBM field solutions along the blade only in terms of local pressure and shear stress vectors. The latter have been integrated to give the Ct and the C_q from which the Figure of Merit is obtained:

$$\text{FoM} = Ct^{1.5}/\left(\sqrt{2}\,Cq\right) \tag{12}$$

Each single point takes roughly 0.2 seconds on a single CPU. Figure 13 right illustrates the contours of the 1076 computed RBMI solutions. Table 5 eventually illustrates the difference in terms of figure of merit for the two targets. The agreement is satisfactory.

	ROSITA FoM	RBMI FoM
Target E (HELISHAPE)	0.5639	0.5604
Target F	0.6316	0.6245

Table 5: Comparison of CFD and RBMI solutions for the Figure of Merit.

5. FINAL REMARKS

The experimentation and numerical simulation of rotor flows are extremely challenging, time-consuming, and costly. Research in rotorcraft aerodynamics tends to rely heavily on both experimental and computational components. In that perspective, the proposed ROM method may constitute a valid support and complement to wind tunnel tests and CFD computations. The assessment of the RBMI method has shown encouraging results in terms of evaluating the complete flow field around an isolated rotor in hover conditions. Even if restricted to steady flow simulations, the present analysis provides encouraging results in view of the application of RBM approaches for the more challenging parametric study of unsteady rotor wakes. Many issues remain open for future research. These involve the definition of more rigorous error estimation and a methodology that allows judicious positioning of the snapshots in the parameter space. From an engineering perspective, it is worth noting that other than giving valid support in the aerodynamic design of rotors, the present methodology may open the way to more refined and accurate flight simulators, where the aerodynamic behavior of the entire rotorcraft is modeled by a real-time RBM computation.

6. REFERENCES

[1] Leishman J., "*Principles of helicopter aerodynamics*", 2nd edition, Cambridge Univ. Press, New York, 2006.

[2] Conlisk A.T., "*Modern helicopter aerodynamics*", Ann. Rev. Fluid Mech., Vol. 29, pp. 515-567, 1998.

[3] Caradonna F.X., Tung C., "*Experimental and analytical studies of a model helicopter rotor in hover*", NASA Technical memorandum 81232, 1981.

[4] Schultz K.J., Splettstoesser W., Junker B., Wagner

W., Schoell E., Arnauld G., Mercker E., Pengel K., Fertis D. "*A parametric wind tunnel test on rotorcraft aerodynamics and aeroacoustics (HELISHAPE). Test documentation and representative results"*, 22nd European Rotorcraft Forum, Brighton, UK, September 1996.

[5] Beaumier P., Costes M., Gaveriaux R., "*Comparison between FP3D full potential calculations and S1 Modane wind tunnel test results on advanced fully instrumented rotors"*, 19th European Rotorcraft Forum, Cernobbio, Italy, September 1993.

[6] Biava M., Khier W., Vigevano L., "CFD prediction of *air flow past a full helicopter configuration*", Aero. Sci. Tech., Vol. 19, pp. 3-18, 2012.

[7] Datta A., Nixon M., Chopra I., "*Review of rotor loads prediction with the emergence of rotorcraft CFD*", Jou. Am. Helicopter Soc., Vol. 52, No. 4, pp. 287–317, 2007.

[8] Pomin H., Wagner S., "*Navier–Stokes analysis of isolated rotor flow in helicopter hover flight*", Proceedings of the European Congress on Computational Methods in Applied Science and Engineering, Barcelona, Spain, Sept. 2000.

[9] Min B.Y., Sankar L.N., "*Hybrid Navier-Stokes/free wake method for modeling blade-vortex interactions*", Jou. Aircraft, Vol. 47, No. 3, pp. 975-982, 2010.

[10] Wachspress D.A., Quackenbush T.R., Boschitsch A.H., "*Rotorcraft interactional aerodynamics with fast vortex/fast panel methods*", Jou. Am. Helicopter Soc., Vol. 48, No. 4, pp. 342-351, 2003.

[11] Beaumier P., Arnaud G., Castellin C., "*Performance prediction and flow field analysis of rotors in hover, using a coupled Euler/boundary layer method"*, Aerosp. Sci. Technol., Vol. 3, pp. 473-484, 1999.

[12] Benoit C., Jeanfaivre G., "*Three–dimensional inviscid isolated rotor calculations using Chimera and automatic Cartesian partitioning methods*", Jou. Am. Helicopter Soc., Vol. 48, pp. 128-138, 2003.

[13] Lucia, D. J., Beran, P. S., Silva, W. A., "Reduced-Order Modeling: New approaches for computational physics," Prog. Aerosp. Sci., Vol. 40, pp. 51–117, 2004.

[14] Antoulas A., Sorensen D., Guercin S., "*A survey of model reduction methods for large-scale systems*", Cont. Mathematics, Chapter 280, AMS: Providence, pp. 193-219, 2001.

[15] Dowell E.H., Hall K.C., Thomas J.P., Florea R., Epureanu B.i., Heeg J., "*Reduced Order models in unsteady aerodynamics*", 40th AIAA/ASME Structures, Structural Dynamics, and Materials Conference and Exhibit, St. Louis, MO, 1999, Collection of Technical Papers. Vol. 1 (A99-24601 05-39), Apr. 1999.

[16] Bui-Thanh T., Willcox K., Ghattas O., "*Model reduction for large-scale systems with high-dimensional parametric input space*", SIAM J. Sci. Comput., Vol. 30, Issue 6, pp. 3270-3288, 2008.

[17] Amsallem D., Cortial J., Farhat C., "*Toward real-time CFD-based aeroelastic computations using a database of reduced-order information*", AIAA J., Vol. 48, Issue 9, pp. 2029-2037, 2010.

[18] Audouze C., De Vuyst F., Nair P.B., "*Reduced Order Modeling of parameterized PDEs using time-space-parameter principal component analysis*", Int. J. Numer. Meth. Eng., Vol. 80, Issue 2, pp. 1025-1057, 2009.

[19] Degroote J., Vierendeels J., Willcox K., "*Interpolation among Reduced Order matrices to obtain parameterized models for design, optimization and probabilistic analysis*", Int. J. Numer. Meth. Fluids, Vol. 63, pp. 207-230, 2010.

[20] Ly H.V., Tran H.T., "*Modeling and control of physical processes using Proper Orthogonal Decomposition*", Math. Comput. Model., Vol. 33, pp. 223-236, 2001.

[21] Bui-Thanh T., Damodaran M., Willcox K., "*Proper Orthogonal Decomposition extensions for parametric applications in transonic aerodynamics*", AIAA Paper 2003-4213, 21st AIAA Applied Aerodynamics Conference, Orlando, Florida, 2003.

[22] Fossati M., Habashi W.G., Baruzzi G.S., "*Simulation of Supercooled Large Droplet impingement via Reduced Order Technology*", Jou. Aircraft, Vol. 49, No. 2, pp. 600-610, 2012.

[23] Fossati M., Habashi W.G., "*Multi-parameter analysis of aero-icing problems via Proper Orthogonal Decomposition and multidimensional interpolation*", AIAA Jou., 2012-02-J051877.R1.

[24] Liu L., Friedmann P.P., Padthe A.K., "An *approximate unsteady aerodynamic model for flapped airfoils including improved drag predictions*", Proceedings of the 34th European Rotorcraft Forum, Liverpool, UK, Sept. 2008.

[25] Glaz B., Liu L., Friedmann, P.P., Bain J., Sankar L.N., "*Surrogate based approach to reduced order dynamic stall modeling*", Jou. Am. Helicopter Soc., Vol. 57, No. 2, 2012.

[26] Suresh S., Omkar S.N., Mani V., Guru-Prakash T.N., "*Lift Coefficient Prediction at High Angle of Attack Using Recurrent Neural Network*", Aerosp. Sci. Technol., Vol. 7, No. 8, pp. 595-602, 2003.

[27] Tang, D., Dowell, E.H. and Peters, D.A., "*Reduced Order aerodynamic models based upon inflow eigenmodes"*, Jou. Am. Helicopter Soc., Vol. 43 No. 4, pp. 342-351, 1998.

[28] Fossati M., Najafiyazdi M., Habashi W.G., "*Mesh adaptation for unsteady problems via Reduced Order Modeling"*, 20th AIAA Computational Fluid Dynamics Conference, Honolulu, HI., AIAA paper 2011-3692, Jul., 2011.

[29] Veroy K., Patera A.T., "Certified real-time solution of the parametrized steady incompressible Navier-Stokes equations: rigorous reduced-basis a posteriori error bounds", Int. J. Numer. Meth. Fluids, Vol. 47, pp. 773-788, 2005.

[30] Du Q., Faber V., Gunzburger M., "*Centroidal Voronoi Tessellations: Applications and algorithms*", SIAM Review, Vol. 41, Issue 4, pp. 637-676, 1999.

[31] Hinze M., Volkwein S., "*Proper Orthogonal*

Decomposition, surrogate models for nonlinear dynamics systems: Error estimates and sub-optimal control", Lecture notes in Computational and Applied Mathematics, Springer-Verlag, Berlin, pp. 201-306, 2005.

[32] Holmes, P., Lumley, J. L., and Berkooz, G., "*Turbulence, coherent structures, dynamical systems and symmetry*", Cambridge University Press, Cambridge, 1996.

[33] Sirovich, L., "*Turbulence and the dynamics of coherent structures: 1 Coherent structures*", Quarterly Appl. Math., Vol. 45, pp. 561-571, 1987.

[34] Akima H., "*A method of bivariate interpolation and smooth surface fitting for irregularly distributed data points*", ACM Transactions on Mathematical Software, Vol. 4 No. 2, pp. 148-159, 1978.

[35] Martin J., Simpson T., "*Use of Kriging models to approximate deterministic computer models*", AIAA Jou., Vol. 43, No. 4, pp. 853-863, 2005.

[36] Forrester A.I.J., Keane A.J., "*Recent advances in surrogate-based optimization*", Progr. Aerosp. Sci., Vol. 45, Issues 1-3, pp. 50-79, 2009.

[37] Roe P.L., "*Approximate Riemann solvers, parameter vectors and difference schemes*", J. Comput. Phys, Vol. 43, pp. 357-372, 1981.

[38] Venkatakrishnan V., "*On the accuracy of limiters and convergence to steady state solutions*", 31st AIAA Aerospace Sciences Meeting and Exhibit, Reno, NV., AIAA 93-0880, 1993.

[39] Jameson A., "*Time dependent calculations using multigrid with applications to unsteady flows past airfoils and wings*", 10th AIAA Computational Fluid Dynamics Conference, Honolulu, HI. AIAA 91-1596, 1991.

[40] Chan W.M., Buning P.G., "*Zipper grids for force and moment computation on overset grids*", AIAA paper 95-1681, 1995.

[41] Chesshire G., Henshaw W.D., "*Composite overlapping meshes for the solution of partial differential equations*", J. Comp. Phys., Vol. 90, pp. 1-64, 1990.

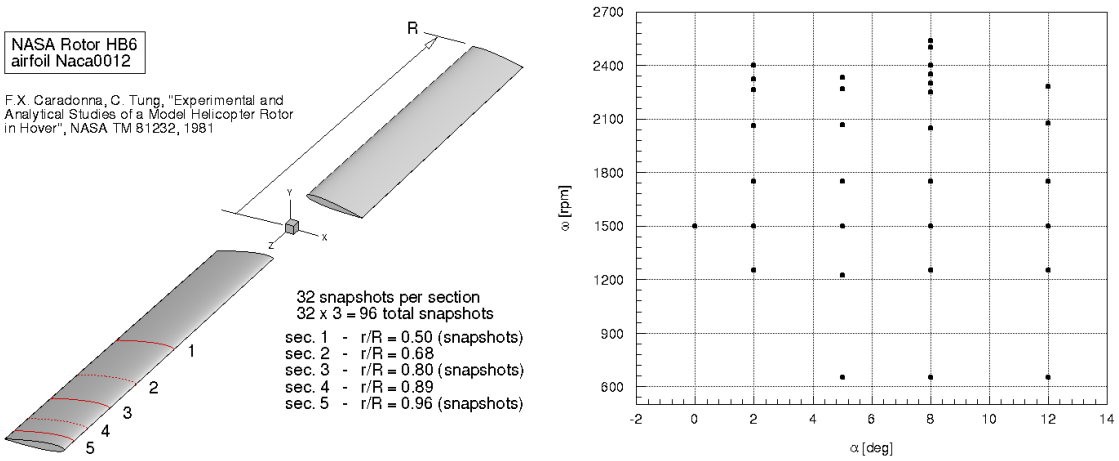

Figure 1: The Caradonna-Tung test case (left), observation arrangement in the parameter space.

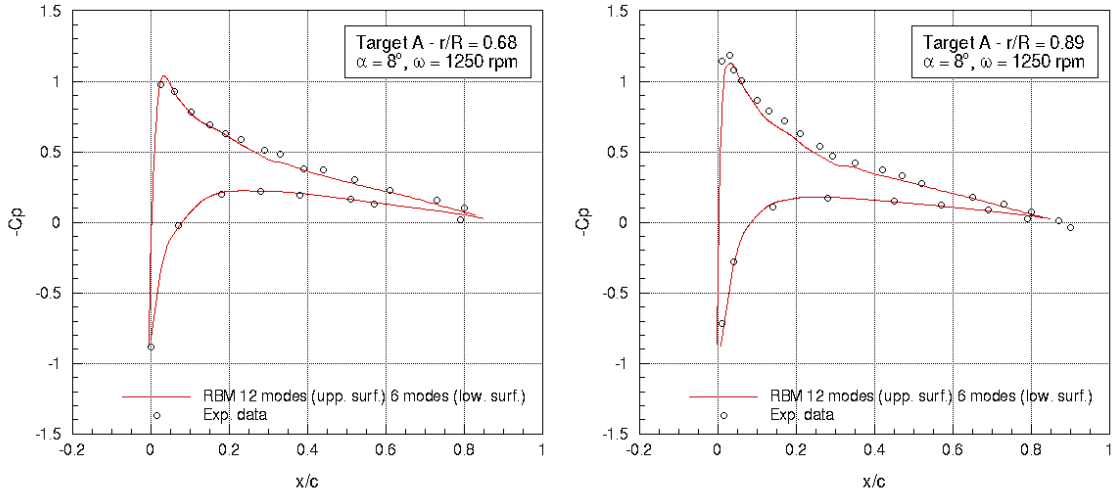

Figure 2: Mock-up simplification. Cp distributions at virtually non-instrumented sections. Target A.

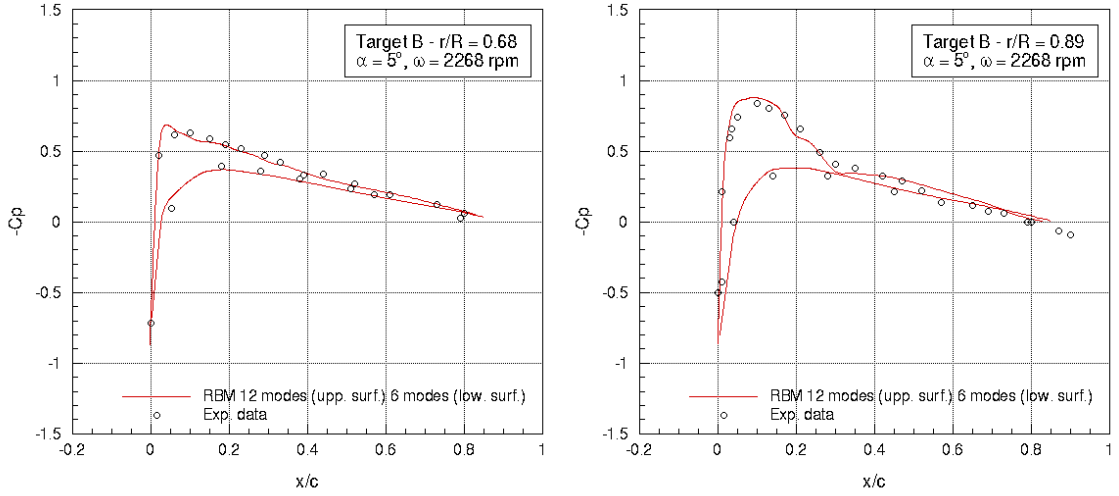

Figure 3: Mock-up simplification. Cp distributions at virtually non-instrumented sections. Target B.

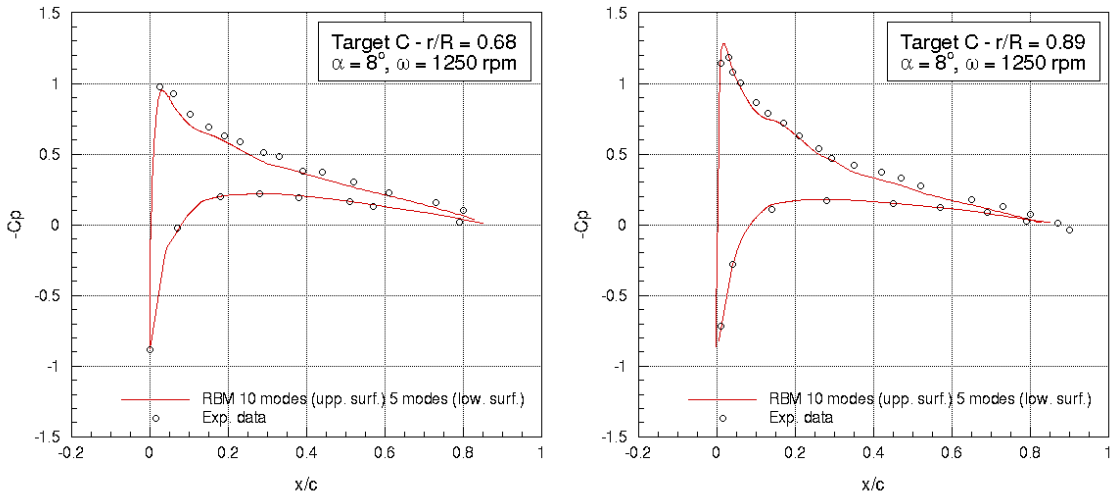

Figure 4: Mock-up simplification and reduction of wind tunnel runs. Target C.

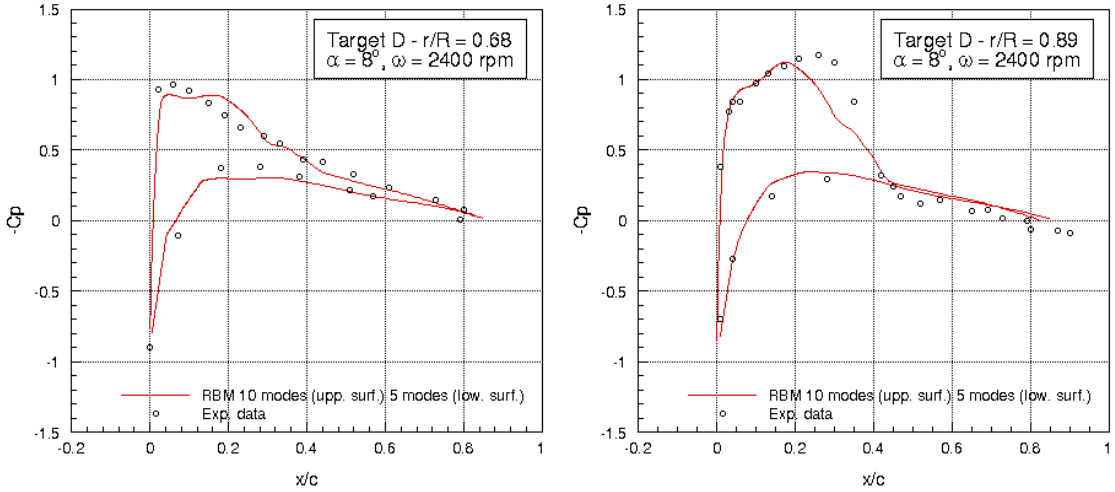

Figure 5: Mock-up simplification and reduction of wind tunnel runs. Target D.

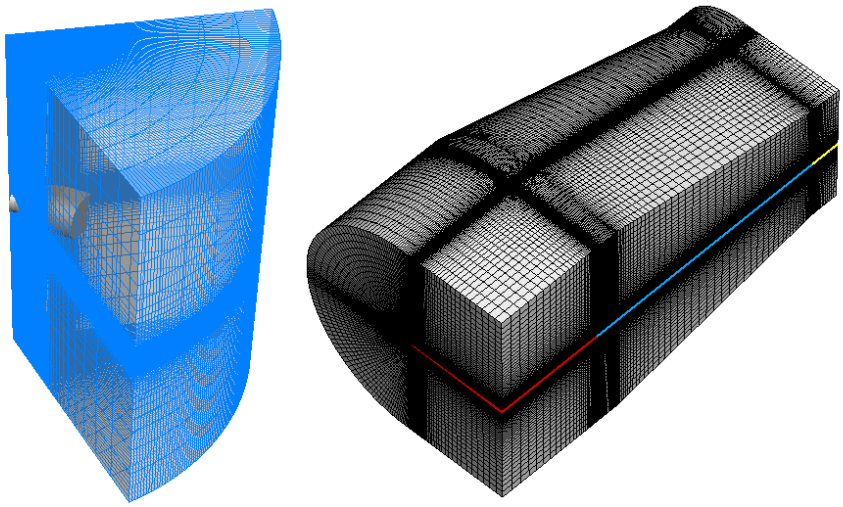

Figure 6: System of multiblock-chimera grids. Background mesh with blades blocks (left), multi-block mesh for the blade (right). Different colors indicate different blocks.

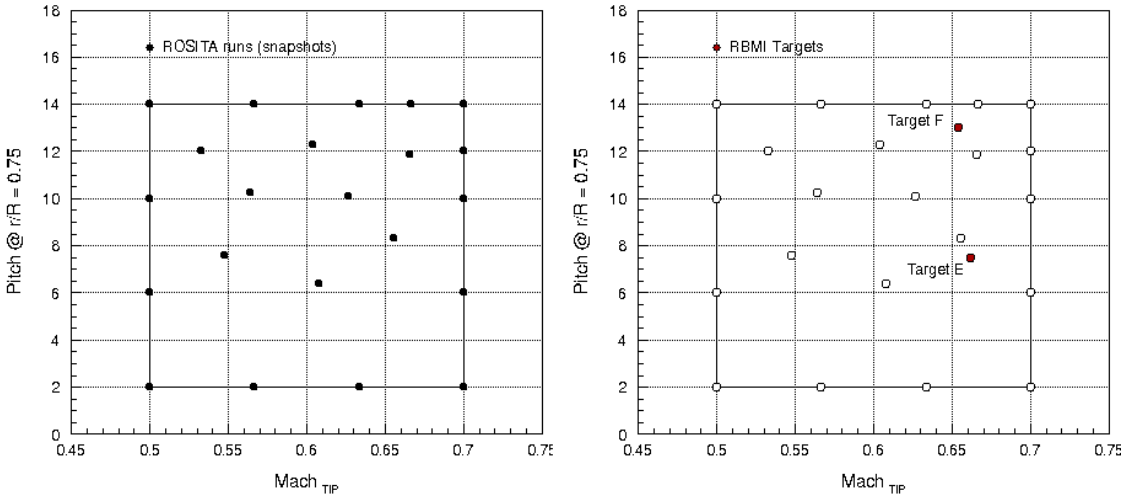

Figure 7: Snapshots arrangement (left), RBM targets (right).

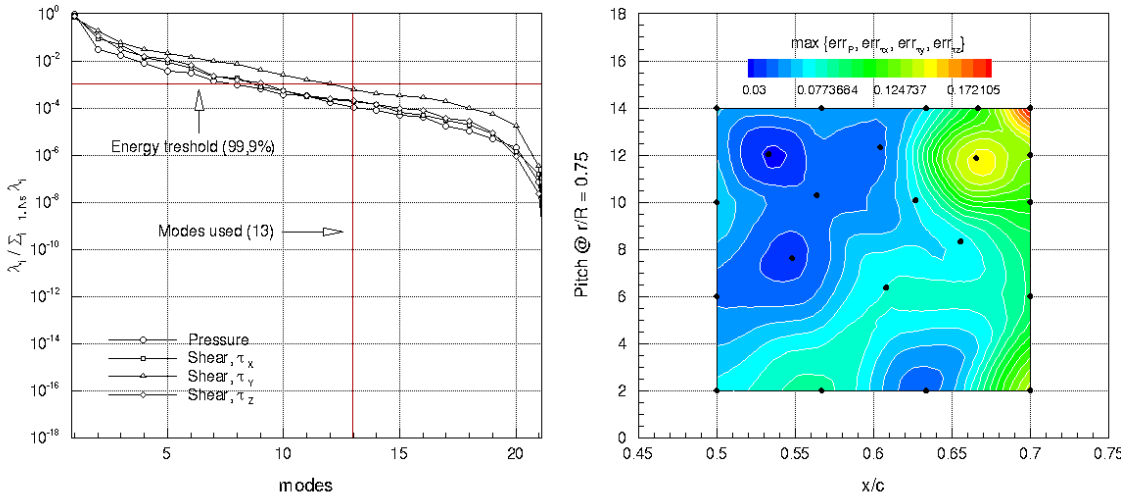

Figure 8: Eigenmodes convergence (left), Leave-out error estimation (right).

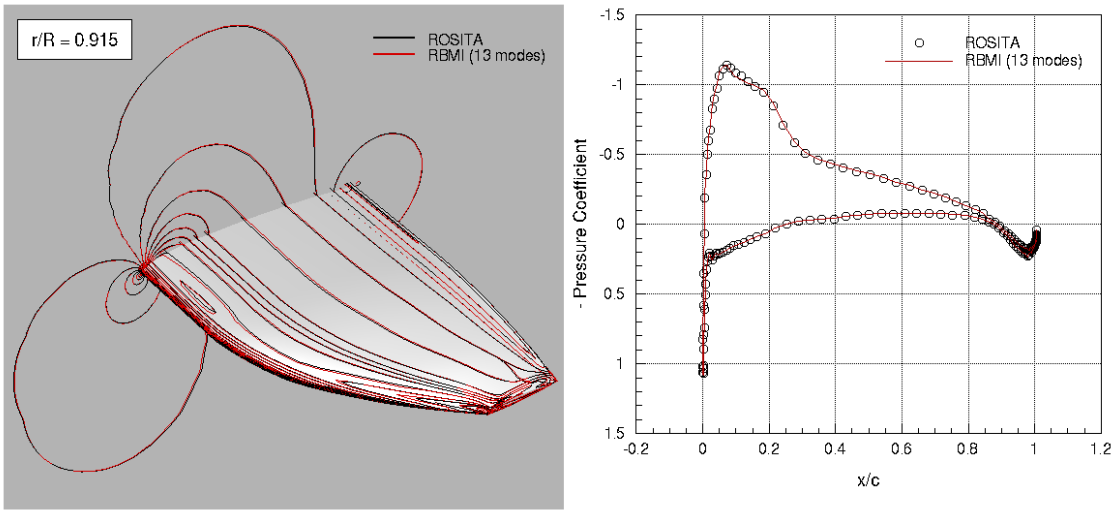

Figure 9: Target E (HELISHAPE). Comparison of Cp distributions (left), Comparison of Cp curves (right).

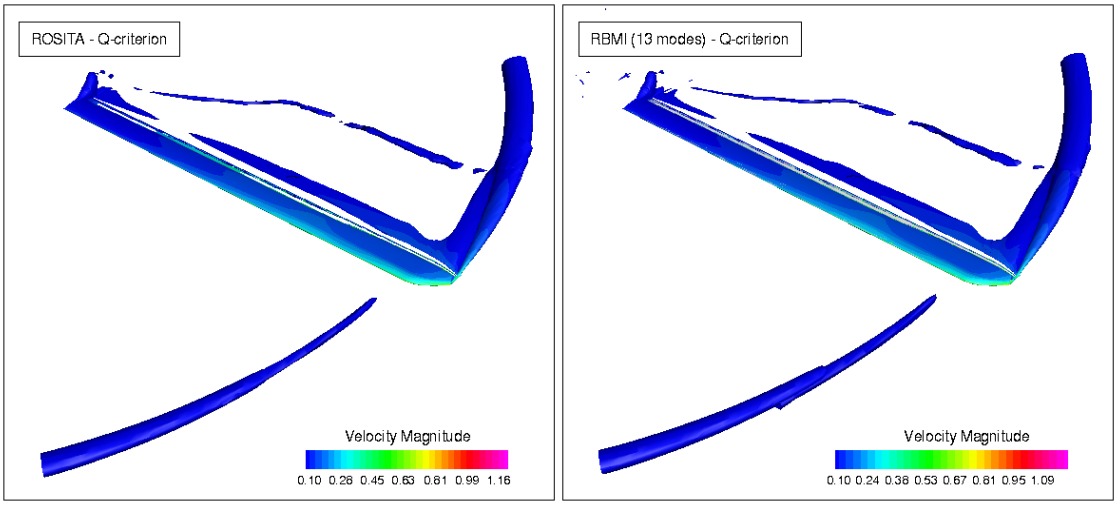

Figure 10: Target A (HELISHAPE). Comparison of Q-criterion. ROSITA (left), RBM (right).

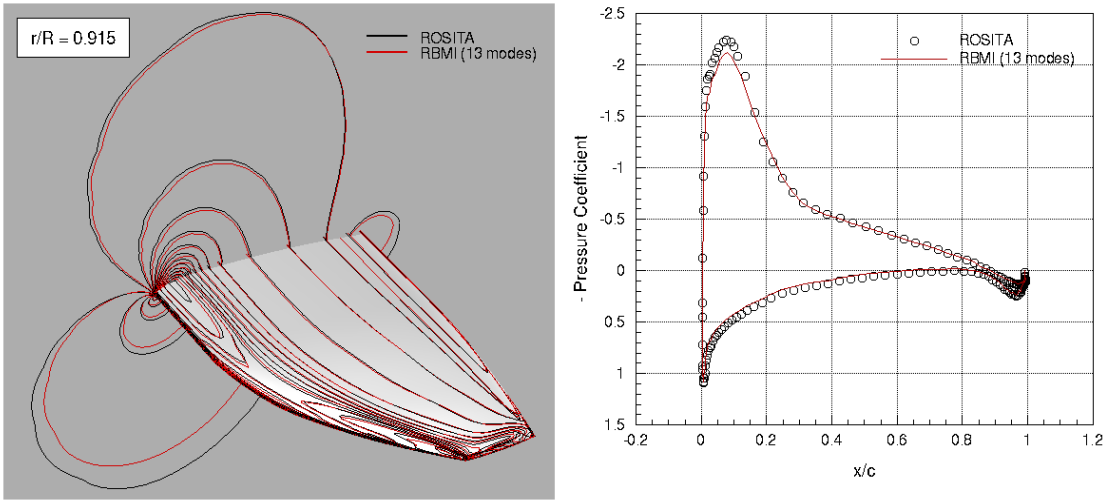

Figure 11: Target B. Comparison of Cp distributions (left), Comparison of Cp curves (right).

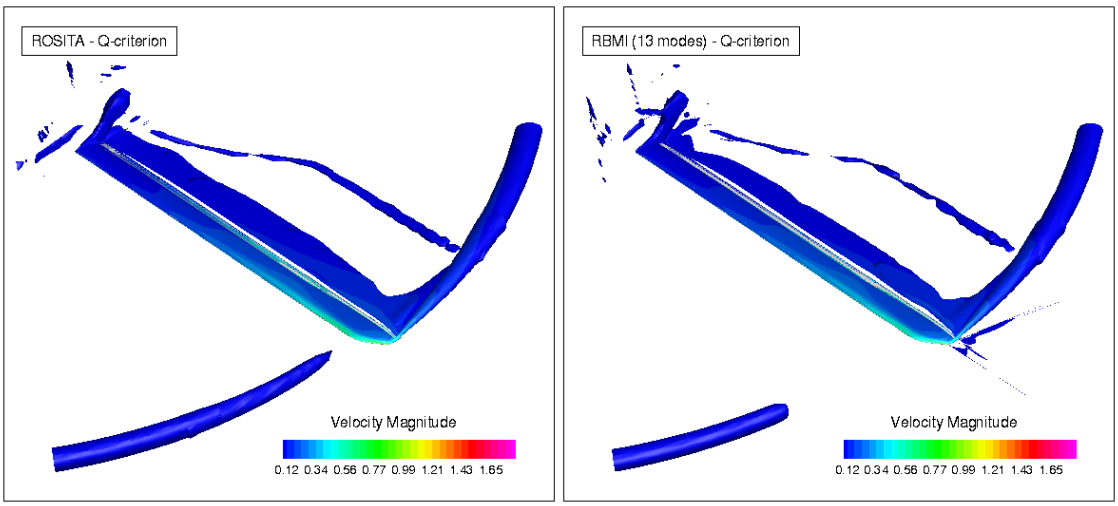

Figure 12: Target B. Comparison of Q-criterion. ROSITA (left), RBMI (right).

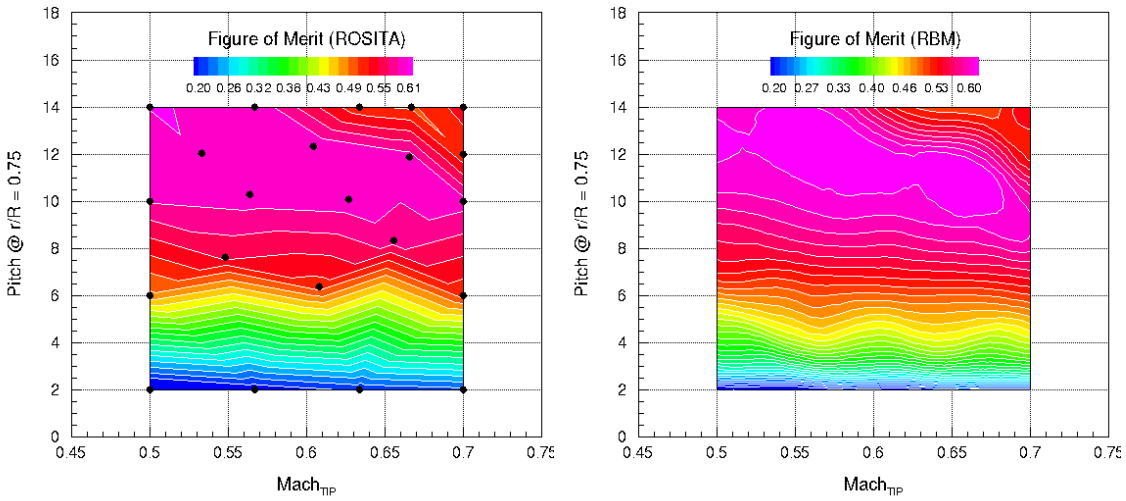

Figure 13: Evaluation of the Figure of Merit via RBMI. ROSITA solution (left), RBMI with 1076 solutions (right).